tvst

Classification of Angle Closure Severity by Hierarchical Cluster Analysis of Ocular Biometrics in the Dark and Light

Austin Cho[1], Juan Pablo Lewinger[1,3], Anmol A. Pardeshi[2], Galo Apolo Aroca[2], Mina Torres[4], Monisha Nongpiur[5], Xuejuan Jiang[2], Roberta McKean-Cowdin[1,3], Rohit Varma[4], and Benjamin Y. Xu[2]

[1] Keck School of Medicine of the University of California, Los Angeles, CA, USA
[2] Roski Eye Institute, Keck School of Medicine, University of Southern California, Los Angeles, CA, USA
[3] Department of Population and Public Health Science, Keck School of Medicine at the University of Southern California, Los Angeles, CA, USA
[4] Southern California Eye Institute, CHA Hollywood Presbyterian Medical Center, Los Angeles, CA, USA
[5] Singapore Eye Research Institute and Singapore National Eye Center, Singapore, Republic of Singapore

Purpose: The purpose of this study was to investigate the classification of angle closure eyes based on hierarchical cluster analysis of ocular biometrics measured in the dark and light using anterior segment optical coherence tomography (AS-OCT).

Methods: Participants of the Chinese American Eye Study received complete eye examinations to identify primary angle closure suspects (PACS) and primary angle closure without/with glaucoma (PAC/G). AS-OCT was performed in the dark and light. Biometric parameters describing the angle, iris, lens, and anterior chamber were analyzed. Hierarchical clustering was performed using Ward's method. Post hoc logistic regression models were developed to identify biometric predictors of angle closure staging.

Results: Analysis of 159 eyes with PACS ($N = 120$) or PAC/G ($N = 39$) produced 2 clusters in the dark and light. In both analyses, cluster 1 ($N = 132$ in the dark and $N = 126$ in the light) was characterized by smaller angle opening distance (AOD)750 and trabecular iris space area (TISA)750, greater iris curvature (IC), and greater lens vault (LV; $P < 0.001$) than cluster 2. The proportion of PAC/PACG to PACS eyes was significantly higher in cluster 1 than 2 in the light (36:90 and 3:30, respectively; $P = 0.02$), but not the dark (36:96 and 3:24, respectively; $P = 0.08$). On multivariable regression analyses, smaller TISA750 (odds ratio [OR] $= 0.84$ per 0.01 mm^2) and AOD750 (OR $= 0.93$ per 0.01 mm) in the light and smaller TISA750 (OR $= 0.86$ per 0.01 mm^2) in the dark conferred higher risk of PAC/G ($P \leq 0.02$).

Conclusions: Unsupervised cluster analysis of ocular biometrics can classify angle closure eyes by severity. Static biometrics measured in the light and dark are both predictive of PAC/G.

Translational Relevance: Clustering of biometrics measured in the light could provide an alternative source of information to risk-stratify angle closure eyes for more severe disease.

Introduction

Primary angle closure glaucoma (PACG) is a leading cause of blindness worldwide.[1,2] Primary angle closure disease (PACD) is a spectrum of disease characterized by appositional or synechial closure of the anterior chamber angle.[3] Angle closure in the form of iridotrabecular contact can impede aqueous flow through the trabecular meshwork, progressing to higher intraocular pressure (IOP) and, in severe cases, PACG.[4] Angle closure is typically categorized

as primary angle closure suspects (PACS), primary angle closure (PAC), and PACG across the spectrum of disease.[5]

Ocular biometric parameters measured using anterior segment optical coherence tomography (AS-OCT) are well-established risk factors in PACD.[6–10] These parameters can also provide information about underlying anatomic mechanisms of angle closure, such as pupillary block, plateau iris configuration, exaggerated lens vault, or thick peripheral iris.[7,11–13] For example, greater iris curvature is believed to reflect increased pupillary block as the pressure increases behind the iris due to resistance to flow through the iris-lens channel, and iris thickness, which can be directly measured in AS-OCT images, directly contributes to higher risk of angle closure.[14,15] Hierarchical cluster analysis, an unsupervised analysis method, also identifies patterns among ocular biometric measurements from angle closure eyes that appear to conform to these broad categories of anatomic mechanisms.[16–19]

Clinical assessments of angle closure risk and underlying anatomic mechanisms are by convention conducted in the dark, as angle width tends to be narrower in the dark than in the light.[20] However, despite strong associations between ocular biometric measurements and the presence of PACD, static measurements under dark lighting conditions appear only moderately predictive of disease stage and progression.[20–22] This raises the question whether biometric data obtained under different static lighting conditions might provide additional information about PACG risk, especially because the majority of waking hours are typically spent in well-lit environments.

In this study, we perform unsupervised hierarchical cluster analysis of biometric data from the Chinese American Eye Study (CHES) to classify eyes with angle closure. The CHES data comprises the full spectrum of PACD in contrast to prior cluster analysis studies of select subsets of angle closure eyes.[16–18] In addition, we analyze biometric data obtained not only in the dark but also the light to identify differences in clustering patterns of biometric parameters and angle closure staging. Although there is limited knowledge about the clinical significance of biometric measurements obtained in the light, we hypothesize that clustering patterns may differ under the two lighting conditions, which could provide novel insights into angle closure mechanisms and severity.

Methods

The CHES was approved by the Ethics Committee from the University of Southern California Medical Center Institutional Review Board. All procedures followed the recommendations of the Declaration of Helsinki. All participants gave informed consent at the time of enrollment. CHES participants were recruited as part of a population-based study on ocular disease in Chinese American individuals aged ≥50 years living in Monterey Park, California.[23] Participants with a history of eye procedures, including laser peripheral iridotomy and cataract surgery, that could affect the anterior segment structures were excluded from this study.

Clinical Examination

Each participant received a complete eye examination by a trained ophthalmologist, including manual gonioscopy and AS-OCT imaging (CASIA SS-1000; Tomey Corporation) in the upright seated position. Gonioscopy was performed under dark ambient lighting (0.1 candela [cd]/m^2) with a 1-mm light beam and a Posner-typer 4-mirror lens (Model ODPSG; Ocular Instruments, Inc.) by a trained ophthalmologist. The angle in each quadrant was graded according to the modified Shaffer classification system: grade 0, no structures visible; grade 1, nonpigmented trabecular meshwork (TM) visible; grade 2; pigmented TM visible; grade 3, scleral spur visible; and grade 4, ciliary body visible. PACD was defined as an eye with ≥3 quadrants gonioscopic angle closure (grade 0 or 1) in the absence of potential causes of secondary angle closure, such as inflammation or neovascularization.

Primary angle closure suspect (PACS) was defined as narrow angles with IOP ≤21 mm Hg without peripheral anterior synechiae (PAS). PAC was defined as PACS with IOP >21 mm Hg or PAS without evidence of glaucomatous optic neuropathy (GON). PACG was defined as PAC with evidence of GON. PAC and PACG eyes were grouped together as PAC/G in the analysis due to the small number of PACG eyes ($N = 5$) in the study cohort.

Anterior Segment Optical Coherence Tomography

AS-OCT imaging of both eyes was performed under dark (0.1 cd/m^2) and light (27 cd/m^2) ambient lighting conditions prior to pupillary dilation. The swept-source SS-OCT viewer software (version 3.0) was used to automatically segment anatomic structures and measure biometric parameters after an experienced grader (author A.P.) manually identified the scleral spur in each image. The grader was masked to the identities and other examination findings of the participants.

translational vision science & technology

One eye per participant was selected for analysis. If both eyes had angle closure, the more severe eye was selected. Otherwise, one eye was selected at random using MATLAB (MathWorks, Natick, MA). Four 2-dimensional radial cross-sectional images, evenly spaced 45 degrees apart with the first image oriented along the horizontal meridian, were analyzed per eye. This approach captures the majority of the anatomic variation along the angle.[24,25] Sectoral measurements were averaged, and these average measurements were further analyzed. Eyes missing measurements from more than three of the eight sectors were excluded from the analysis.

Two biometric parameters describing angle width were measured: angle opening distance (AOD) and trabecular iris space area (TISA). AOD750 was defined as the perpendicular distance from the TM at 750 μm anterior to the scleral spur to the anterior iris surface. TISA750 was defined as the area bounded anteriorly by AOD750; posteriorly by a line drawn from the scleral spur perpendicular to the plane of the inner scleral wall to the opposing iris; superiorly by the inner corneoscleral wall; and inferiorly by the iris surface. Iris area (IA), anterior chamber depth (ACD), iris curvature (IC), lens vault (LV), and anterior chamber width (ACW) were also measured.[26,27] IA was defined as the cross-sectional area of the full length of the iris. ACD was defined as the distance from the apex of the anterior lens surface to the apex of the corneal endothelium. IC was defined as the distance from the apex of the iris convexity to a line extending from the peripheral to central iris pigment epithelium. ACW was defined as the distance between scleral spurs. Pupil diameter (PD) was defined as the shortest distance between the edges of the pupil. Intra-grader measurement repeatability was previously assessed and reported to be excellent for all parameters, with intraclass correlation coefficients (ICCs) ranging from 0.89 to 0.98.[20] Detection of the scleral spur has been previously assessed and shown to have excellent intragrader and intergrader reproducibility.[28]

Statistical Analysis

Continuous and categorical variables were summarized as mean ± standard deviation (SD) and proportions, respectively. Distributions of continuous variables were compared using the two-sample *t*-test or Wilcoxon signed rank test depending on the result of normality testing using the Shapiro-Wilk test. Proportions of categorical variables were compared using the Chi-squared test. Hierarchical cluster analysis was used to classify PACD eyes. Measurements of each parameter were standardized (values subtracted by

mean and then divided by SD) prior to analysis so as not to affect squared Euclidean distances. Agglomerative cluster analysis was performed using Euclidean distance as the similarity measure and Ward's method as the clustering algorithm. Each case started with each cluster as a separate cluster; clusters were then combined until only one cluster remained. Cluster analysis was applied using squared Euclidean distances as a similarity measure and Ward's method as the clustering algorithm. The Duda-Hart (DH) index and pseudo t^2 statistics (PST2) were used to determine the optimal number of clusters. The DH index utilizes the ratio of the two within sum of squares to decide if a cluster can be divided into separate clusters. PST2 is derived from the DH index and accounts for the total number of cases. The optimal number of clusters was chosen by selecting the number of clusters corresponding to the highest DH index value and a correspondingly low PST2 value. The clustering method was validated by randomly splitting the entire dataset into two datasets with similar proportions of PACS and PAC/G eyes and repeating the clustering analysis on each dataset. Univariable logistic regression analysis was performed with dark and light AS-OCT parameters as independent variables and disease stage (PACS or PAC/PACG) as the dichotomous outcome variable. Multivariable logistic regression analysis included age, sex, and all parameters with *P* values < 0.2 on univariable analysis. AOD750 and TISA750 were not included in the same regression model due to collinearity. Area under the receiver operating curve (AUC) metrics were calculated to assess predictive performance of regression models. All analyses were performing using the R software version 4.2.1 (R Foundation for Statistical Computing, Vienna, Austria). Statistical analyses were conducted using a significance level of 0.05.

Results

AS-OCT data was available on 169 eyes of 169 participants with PACS or PAC/G. After excluding 10 participants with a history of intraocular surgery or laser peripheral iridotomy (LPI), 159 eyes were eligible for analysis, all of which had biometric data from 5 or more sectors. One hundred twenty eyes had PACS and 39 participants had PAC/G. Mean age was 61.7 ± 7.79, mean IOP was 16.2 ± 3.49, and 122 (76.7%) of the participants were women. The optimal number of clusters was 2 for both dark and light measurements based on DH index and PST2.

In the dark analysis, there were 132 eyes in cluster 1 and 27 eyes in cluster 2 (Table 1, see the Fig.).

Table 1. Comparison of Demographics and Ocular Biometric Factors Between Clusters 1 and 2 From the 2-Cluster Analysis

Lighting	Mean Parameters (Mean ± SD)	Cluster 1	Cluster 2	P Value[a]
Dark		$N = 132$	$N = 27$	
	Sex (F:M)[b]	100:32	22:5	0.52
	Age, y[b]	62.3 ± 7.87	58.8 ± 6.78	**0.03**
	IOP[b] (mm Hg)	16.368 ± 3.616	15.321 ± 2.688	0.14
	PAC/G:PACS[c]	36:96	3:24	0.08
	AOD750 (mm)	0.157 ± 0.051	0.225 ± 0.055	**<0.001**
	TISA750 (mm^2)	0.088 ± 0.034	0.114 ± 0.024	**<0.001**
	IA (mm^2)	1.611 ± 0.213	1.554 ± 0.213	0.24
	IT750 (mm)	0.398 ± 0.080	0.425 ± 0.052	**0.02**
	IC (mm)	0.297 ± 0.060	0.206 ± 0.060	**<0.001**
	ACD (mm)	2.137 ± 0.195	2.420 ± 0.184	**<0.001**
	LV (mm)	0.838 ± 0.157	0.573 ± 0.136	**<0.001**
	ACW (mm)	11.509 ± 0.195	11.454 ± 0.281	0.49
	PD (mm)	3.670 ± 0.657	4.259 ± 0.880	**<0.001**
Light		$N = 126$	$N = 33$	
	Sex[b] (F:M)	98:28	24:9	0.54
	Age,[b] y	62.1 ± 8.26	60.5 ± 5.61	0.66
	IOP[b] (mm Hg)	16.306 ± 3.557	15.747 ± 3.236	0.36
	PAC/G:PACS[c]	36:90	3:30	**0.02**
	AOD750 (mm)	0.218 ± 0.054	0.311 ± 0.047	**<0.001**
	TISA750 (mm^2)	0.126 ± 0.034	0.164 ± 0.026	**<0.001**
	IA (mm^2)	1.811 ± 0.221	1.888 ± 0.218	**0.08**
	IT750 (mm)	0.339 ± 0.065	0.332 ± 0.046	0.58
	IC (mm)	0.301 ± 0.072	0.256 ± 0.056	**<0.001**
	ACD (mm)	2.101 ± 0.168	2.464 ± 0.142	**<0.001**
	LV (mm)	0.867 ± 0.158	0.656 ± 0.124	**<0.001**
	ACW (mm)	11.483 ± 0.375	11.685 ± 0.362	**0.006**
	PD (mm)	2.553 ± 0.592	2.567 ± 0.351	0.32

ACD, anterior chamber depth; ACW, anterior chamber width; AOD, angle opening distance; IA, iris area; IC, iris curvature; IOP, intraocular pressure; IT, iris thickness; LV, lens vault; PAC, primary angle closure; PACS, primary angle closure suspect; PACG, primary angle closure glaucoma; PD, pupillary diameter; TISA, trabecular iris surface area.

[a]Statistical significance tested by Wilcoxon *t*-test or two-sample *t*-test.
[b]Post hoc; not included in cluster analysis.
[c]Statistical significance tested by Chi-squared test.

Cluster 1 was significantly ($P = 0.03$) older than cluster 2 (62.3 ± 7.9 and 58.8 ± 6.8 years, respectively). Clusters 1 and 2 had similar IOP (16.34 ± 3.6 and 15.3 ± 2.7 mm Hg, respectively; $P = 0.14$) and proportion of women overall (75.8% and 81.4%, respectively; $P = 0.52$). Cluster 1 had smaller AOD750 and TISA750 and greater IC and LV ($P < 0.001$; see Table 1). Cluster 2 had greater ACD and PD ($P < 0.001$). There was no significant difference ($P = 0.08$) in the proportion of PAC/G between clusters 1 (36 out of 132; 27.3%) and 2 (3 out of 27; 11.1%) in the dark analysis.

In the light analysis, cluster 1 had 126 eyes and cluster 2 had 33 eyes (see Table 1, the Fig.). No significant difference was found ($P = 0.66$) in age between cluster 1 and cluster 2 (62.1 ± 8.3 and 60.5 ± 5.6 years, respectively). Clusters 1 and 2 had similar IOP (16.3 ± 3.6 and 15.7 ± 3.2, respectively; $P = 0.36$) and proportion of women overall (77.8% and 72.7%; $P = 0.54$). Cluster 1 had smaller AOD750 and TISA ($P < 0.001$), smaller ACW ($P = 0.01$), and greater IC and LV ($P < 0.001$; see Table 1). Cluster 2 had greater ACD ($P < 0.001$). There was a significantly greater ($P = 0.02$) proportion of PAC/G in cluster 1 (36 out of 126; 28.6%) compared to cluster 2 (3 out 33; 9.1%) in the light analysis.
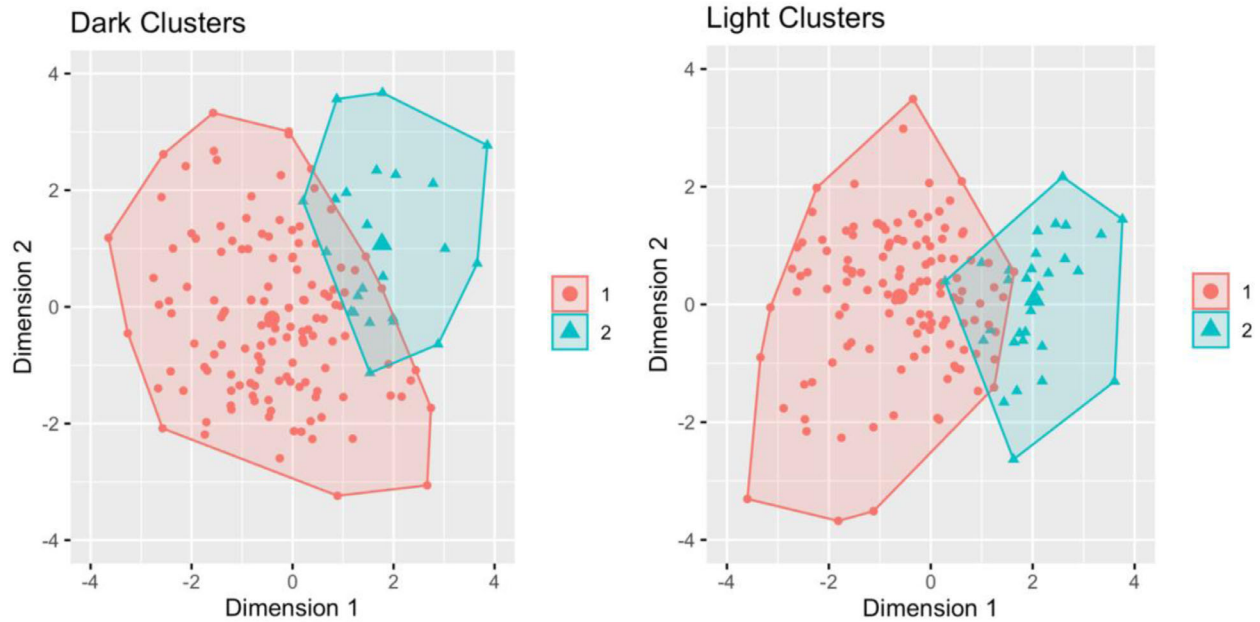
Figure. Clustering of AS-OCT measurements from PACD eyes in the dark (*left*) and light (*right*).

Table 2. Number of Eyes That Switched Clusters Between Dark and Light Analyses

Clusters	PACS	PAC/G	Total #
Cluster 1 only (dark and light)	85	34	119
Cluster 2 only (dark and light)	19	1	20
Cluster 1 (dark) to cluster 2 (light)	11	2	13
Cluster 2 (dark) to cluster 1 (light)	5	2	7

PAC, primary angle closure; PACS, primary angle closure suspect; PACG, primary angle closure glaucoma.

In an analysis of change in cluster between dark and light, cluster identity was mostly conserved across lighting conditions (Table 2). Thirteen eyes (8.2% of total; 11 PACS and 2 PAC/G) changed from cluster 1 in the dark analysis to cluster 2 in the light analysis. Seven eyes (4.4% of total; 5 PACS and 2 PAC/G) changed from cluster 2 in the dark analysis to cluster 1 in the light analysis.

A sensitivity analysis conducted with three instead of two clusters produced similar results (Supplementary Table S1, Supplementary Fig. S1). In the dark analysis, cluster 1 (71) was characterized by smaller AOD750 and TISA750; cluster 2 (61) was characterized by greater IC and LV; and cluster 3 (27) was characterized by greater ACD, IT, and PD. In the light analysis, cluster 1 (16) was characterized by smaller AOD750 and TISA750, ACW, and PD; cluster 2 (110) was characterized by greater IC; and cluster 3 (33) was characterized by greater ACD. Similar to the 2-cluster analysis, there was a significant inter-cluster difference in proportion of PAC/G to PACS among clusters 1, 2, and 3 in the light analysis (8:8, 28:82, and 3:30, respectively; $P = 0.01$), but not in the dark analysis (23:48, 13:48, and 3:24, respectively; $P = 0.07$).

Post hoc logistic regression analysis was performed to identify which parameter/s within each cluster was contributing to the observed difference in angle closure staging. On univariable analysis, only greater TISA750 in the dark (odds ratio [OR] = 0.86 per 0.01 mm^2) and light (OR = 0.84 per 0.01 mm^2) and greater AOD750 in the light (OR = 0.93 per 0.01 mm) were significantly associated ($P = 0.02$) with lower odds of PAC/G (Table 3). On multivariable logistic regression analysis of eligible parameters measured in the light, greater TISA750 (OR = 0.85 per 0.01 mm^2) was significantly associated ($P = 0.007$) with lower odds of PAC/G after adjusting for age and sex (AUC = 0.681, 95% confidence interval [CI] = 0.573–0.788). Greater AOD750 (OR = 0.93 per 0.01 mm) in the light was also significantly associated ($P = 0.04$) with lower odds of PAC/G in a separate multivariable model with similar covariates (AUC = 0.641, 95% CI = 0.538–0.744). TISA750 was the only parameter measured in the dark eligible for multivariable logistic regression analysis; greater TISA750 (OR = 0.85 0.01 per mm^2) remained associated ($P = 0.01$) with lower odds of PAC/G after adjusting for age and sex (AUC = 0.628, 95% CI = 0.525–0.782).

Table 3. Univariable and Multivariable Logistic Regression Analysis of Demographic and Ocular Biometric Factors Associated With PAC/G

Lighting	Parameter	PACS Mean (SD)	PAC/G Mean (SD)	Univariable Analysis		Multivariable Analysis	
				OR (CI)	*P* Value	OR (CI)	*P* Value
Light	Age, y	61.2 (7.9)	63.3 (7.3)	1.03 (0.99-1.08)	0.16	1.03 (0.98-1.08)	0.25
	Sex						
	Female	96 (78.7)	26 (21.3)	REF		REF	
	Male	24 (64.9)	13 (35.1)	2.00 (0.88-4.43)	0.09	1.82 (0.76-4.24)	0.17
	AOD750 (mm)	24.4 (6.3)	21.5 (6.7)	**0.93 (0.87-0.98)**	**0.02**		
	TISA750 (mm^2)	13.9 (3.3)	11.7 (4.0)	**0.84 (0.75-0.93)**	**0.002**	**0.85 (0.75-0.95)**	**0.007**
	IA (mm^2)	18.4 (2.2)	17.8 (2.4)	0.88 (0.74-1.03)	0.12	0.90 (0.72-1.12)	0.36
	IT750 (mm)	3.4 (0.6)	3.4 (0.6)	1.00 (0.55-1.78)	0.99		
	IC (mm)	2.9 (0.7)	2.9 (0.8)	0.90 (0.55-1.51)	0.69		
	ACD (mm)	21.9 (2.2)	21.4 (2.0)	0.91 (0.76-1.07)	0.26		
	LV (mm)	8.1 (1.8)	8.6 (1.7)	1.16 (0.94-1.44)	0.16	1.10 (0.88-1.39)	0.42
	ACW (mm)	11.5 (0.4)	11.5 (0.3)	0.77 (0.30-2.00)	0.59		
	PD (mm)	2.5 (0.5)	2.7 (0.6)	1.57 (0.83-3.00)	0.16	0.95 (0.39-2.31)	0.91
Dark	Age, y	61.2 (7.9)	63.3 (7.3)	1.03 (0.99-1.08)	0.16	1.04 (0.99-1.10)	0.08
	Sex						
	Female	96 (80.0)	26 (66.7)	REF		REF	
	Male	24 (20.0)	13 (33.3)	2.00 (0.88-4.43)	0.90	2.05 (0.88-4.70)	0.091
	AOD750 (mm)	17.2 (5.7)	15.7 (5.9)	0.95 (0.89-1.02)	0.15		
	TISA750 (mm^2)	9.6 (3.4)	8.0 (3.3)	**0.86 (0.76-0.97)**	**0.01**	0.85 (0.75-0.95)	**0.006**
	IA (mm^2)	16.1 (2.1)	15.8 (2.3)	0.93 (0.78-1.10)	0.41		
	IT750 (mm)	4.0 (0.8)	4.1 (0.8)	1.08 (0.66-1.71)	0.75		
	IC (mm)	2.8 (0.7)	2.7 (0.7)	0.77 (0.45-1.31)	0.33		
	ACD (mm)	22.0 (2.3)	21.5 (1.9)	0.91 (0.76-1.07)	0.27		
	LV (mm)	7.8 (1.9)	8.2 (1.6)	1.11 (0.91-1.37)	0.30		
	ACW (mm)	11.5 (0.4)	11.5 (0.3)	0.70 (0.26-1.82)	0.46		
	PD (mm)	3.8 (0.7)	3.8 (0.7)	1.05 (0.64-1.72)	0.84		

Statistically significant *P* values and odds ratios are bolded.

OR, odds ratio; CI, confidence interval; ACD, anterior chamber depth; ACW, anterior chamber width; AOD, angle opening distance; IA, iris area; IC, iris curvature; IOP, intraocular pressure; IT, iris thickness; LV, lens vault; PAC, primary angle closure; PACS, primary angle closure suspect; PACG, primary angle closure glaucoma; PD, pupillary diameter; TISA, trabecular iris surface area.

Discussion

In this study, hierarchical cluster analysis of biometric measurements from Chinese American eyes with angle closure revealed two clusters under both light and dark conditions. Clusters in dark and light analyses both appeared to segregate based primarily on established biometric risk factors for PACD. Although cluster 1 had a significantly higher proportion of PAC/G than cluster 2 in the light, inter-cluster difference in proportions was not significantly different in the dark. Post hoc logistic regression analysis showed that smaller TISA750 and AOD750 in the light and TISA750 in the dark were significantly associated with PAC/G. These findings based on unsupervised analysis of angle closure eyes provide potential insights into anatomic mechanisms and the role of biometric measurements obtained in the light to risk stratify participants for PAC/G.

Our cluster analysis produced two clusters in both the light and dark analyses, similar to cluster analyses of PACD eyes conducted by Baek et al. and Nongpiur et al.[16,18] Similar to those studies, clusters in our study did not appear cleanly grouped by angle closure subtype (e.g. pupillary block, plateau iris configuration, and thick peripheral iris roll). Instead, biometric factors that are associated with PAC/G were generally grouped together.[16,18] Cluster 1 in both dark and light analyses were characterized by narrower angles,

greater IC and LV, and smaller ACD, which are well-established biometric risk factors for PACD.[6,7,9] It is tempting to further subcategorize the clusters into angle closure subtypes; increased IC has been previously reported as an indicator of pupillary block, and flatter IC and deeper ACD are associated with plateau iris configuration.[29–31] However, this type of subclassification should be performed cautiously as angle closure subtypes cannot be confirmed with existing CHES data (e.g. ultrasound biomicroscopy [UBM] was not performed to confirm plateau iris configuration), and it is difficult to ascertain why the unsupervised cluster analysis grouped eyes together in the way it did. Therefore, we believe it is only appropriate to conclude that cluster analysis appears to segregate PACD eyes in CHES by factors that are known to increase risk of angle closure.

Cluster analysis of biometric measurements in CHES appeared to identify subpopulations of eyes with a higher proportion of PAC/G, a finding that is consistent across two or three clusters. This finding highlights a novel difference between our study, which includes PACS and PAC/G eyes, and studies by Baek et al., which only included patients with PAC/G, and Nongpiur et al., which only included either PACS or PAC/G eyes in two separate cluster analyses.[16–18] Specifically, when eyes that span the entire spectrum of angle closure are clustered together, classification appears to occur by severity. Our cohort also differs from that of Moghimi et al., which included a substantial proportion (nearly half) of acute primary angle closure (APAC) and fellow APAC eyes.[19] This difference may explain why their analysis produced three clusters, with one cluster comprised almost entirely of APAC and fellow APAC eyes. These differences in results between studies suggest that this type of clustering analysis, and by extension inferences about its results, may be specific to the study cohort.

The identification of a subpopulation of eyes with a higher proportion of PAC/G is clinically significant in the setting of the Zhongshan Angle-Closure Prevention (ZAP) Trial and Singapore Asymptomatic Narrow Angles Laser Iridotomy Study (ANA-LIS), which both reported low risk of progression from PACS to PAC.[32,33] These studies highlight the importance of developing novel methods to risk-stratify PACS eyes for more severe angle closure and identify eyes that could benefit from prophylactic treatment with LPI. While is tempting to speculate that PACS eyes in cluster 2 may be at higher risk of developing PAC/G than in cluster 1, it is important to point out that our findings are based on cross-sectional data that could be confounded by unobserved factors. Therefore, cluster analysis of data from longitudinal studies

like the ZAP Trial and ANA-LIS may help establish the relative prognostic value of clustering biometric measurements for predicting angle closure progression starting from a common baseline.

Cluster analysis of biometric measurements from the light but not the dark segregated eyes into groups with significantly higher (cluster 1; 29% probability) or lower (cluster 2, 9% probability) proportions of eyes with PAC/G. Although the measurements of most biometric parameters differed between clusters 1 and 2 in the light, it is unclear which parameters contributed to the difference in angle closure staging based solely on the unsupervised cluster analysis. This led us to perform post hoc logistic regression analysis of biometric measurements as risk factors for PAC/G, which showed that angle width parameters were the most significant predictors of angle closure staging. This finding is consistent with previous studies that support the primary role of angle width in determining angle closure severity and progression risk.[6,29,34] Comparison of biometric measurements from clusters 1 and 2 in the dark showed some of the same differences as in the light; however, the difference in proportions of eyes with PAC/G (27% and 13%, respectively) did not reach statistical significance, which may be an effect of the relatively small sample size of PAC/G eyes in our cohort. A similar difference in significance was observed when three-cluster analysis was performed on dark and light data. In addition, only TISA750 and not AOD750 was associated with PAC/G in the dark. Finally, the AUC of TISA750 trended toward being higher in the light (AUC = 0.681) than in the dark (AUC = 0.628). These findings together suggest that angle parameters measured outside of the dark provide an alternative source of information about PAC/G risk that could be used to stratify angle closure eyes, which to our knowledge has not been previously shown.[20]

Our study has several limitations. First, we did not separate eyes with PAC and PACG due to the relatively small number ($N = 15$) of PACG cases in the CHES cohort. We also did not have sufficient data to identify eyes with prior episodes of acute angle closure (AAC). Therefore, we were unable to assesses differences in clustering patterns within these angle closure subtypes. Second, we analyzed biometric measurements averaged across eight sectors of the eye. Whereas this approach better captures anatomic variations of the angle, it may weaken the effect of specific sectors that are more predictive of disease stage or progression, such as the temporal and nasal sectors.[24,25] A more thorough investigation of these factors in the future may help elucidate differences in PAC/G in the light and dark. Third, the number of PAC/G eyes in CHES is small, which could limit the ability of

the clustering algorithm to stratify this cohort. Future study of a larger dataset with more PACS and PAC/G eyes may yield additional insights into identifying eyes at higher risk for PACG. Finally, CHES participants all self-identified as Chinese American. Therefore, the study results may not generalize to other populations. However, generalizability may be improved compared to prior community and hospital-based studies.[16–19]

In conclusion, hierarchical cluster analysis appears to classify angle closure eyes by stage when applied to biometric measurements that comprise the full spectrum of disease. In addition, measurements obtained in the light may provide useful information about angle closure staging even though clinical assessments of the anterior chamber angle are by convention performed in the dark. Although clustering of biometric measurements obtained in the light may provide an alternative method to risk-stratify angle closure eyes for more severe disease, longitudinal studies using quantitative OCT measurements to predict angle closure outcomes are needed to validate this approach.

Acknowledgments

Disclosure: **A. Cho**, None; **J.P. Lewinger**, None; **A.A. Pardeshi**, None; **G.A. Aroca**, None; **M. Torres**, None; **M. Nongpiur**, None; **X. Jiang**, None; **R. McKean-Cowdin**, None; **R. Varma**, None; **B.Y. Xu**, None

References

1. Quigley H, Broman AT. The number of people with glaucoma worldwide in 2010 and 2020. *Br J Ophthalmol*. 2006;90(3):262–267.
2. Tham YC, Li X, Wong TY, Quigley HA, Aung T, Cheng CY. Global prevalence of glaucoma and projections of glaucoma burden through 2040: a systematic review and meta-analysis. *Ophthalmology*. 2014;121(11):2081–2090.
3. Primary Angle-Closure Disease PPP 2020 - American Academy of Ophthalmology. Accessed September 27, 2022. Available at: https://www.aao.org/preferred-practice-pattern/primary-angle-closure-disease-ppp.
4. Weinreb RN, Aung T, Medeiros FA. The pathophysiology and treatment of glaucoma: a review. *JAMA*. 2014;311(18):1901–1911.
5. Foster PJ, Buhrmann R, Quigley HA, Johnson GJ. The definition and classification of glaucoma in prevalence surveys. *Br J Ophthalmol*. 2002;86(2): 238–242.
6. Xu BY, Friedman DS, Foster PJ, et al. Ocular biometric risk factors for progression of primary angle closure disease: the zhongshan angle closure prevention trial. *Ophthalmology*. 2022;129(3):267–275.
7. Nongpiur ME, He M, Amerasinghe N, et al. Lens vault, thickness, and position in Chinese subjects with angle closure. *Ophthalmology*. 2011;118(3):474–479.
8. Nongpiur ME, Sakata LM, Friedman DS, et al. Novel association of smaller anterior chamber width with angle closure in Singaporeans. *Ophthalmology*. 2010;117(10):1967–1973.
9. Aung T, Nolan WP, Machin D, et al. Anterior chamber depth and the risk of primary angle closure in 2 East Asian populations. *Arch Ophthalmol*. 2005;123(4):527–532.
10. Shan J, DeBoer C, Xu BY. Anterior segment optical coherence tomography: applications for clinical care and scientific research. *Asia-Pac J Ophthalmol Phila Pa*. Published online April 25, 2019, doi:10.22608/APO.201910.
11. Shabana N, Aquino MC, See J, et al. Quantitative evaluation of anterior chamber parameters using anterior segment optical coherence tomography in primary angle closure mechanisms. *Clin Experiment Ophthalmol*. 2012;40(8):792–801.
12. Wang N, Wu H, Fan Z. Primary angle closure glaucoma in Chinese and Western populations. *Chin Med J*. 2002;115(11):1706–1715.
13. He M, Foster PJ, Johnson GJ, Khaw PT. Angle-closure glaucoma in East Asian and European people. Different diseases? *Eye 2006 201*. 2005;20(1):3–12.
14. Guzman CP, Gong T, Nongpiur ME, et al. Anterior segment optical coherence tomography parameters in subtypes of primary angle closure. *Invest Ophthalmol Vis Sci*. 2013;54(8):5281–5286.
15. Wang BS, Narayanaswamy A, Amerasinghe N, et al. Increased iris thickness and association with primary angle closure glaucoma. *Br J Ophthalmol*. 2011;95(1):46–50.
16. Nongpiur ME, Gong T, Lee HK, et al. Subgrouping of primary angle-closure suspects based on

anterior segment optical coherence tomography parameters. *Ophthalmology*. 2013;120(12):2525–2531.

17. Nongpiur ME, Atalay E, Gong T, et al. Anterior segment imaging-based subdivision of subjects with primary angle-closure glaucoma. *Eye 2017 314*. 2016;31(4):572–577.

18. Baek S, Sung KR, Sun JH, et al. A hierarchical cluster analysis of primary angle closure classification using anterior segment optical coherence tomography parameters. *Invest Ophthalmol Vis Sci*. 2013;54(1):848–853.

19. Moghimi S, Torkashvand A, Mohammadi M, et al. Classification of primary angle closure spectrum with hierarchical cluster analysis. *PLoS One*. 2018;13(7):e0199157, doi:10.1371/JOURNAL.PONE.0199157

20. Lifton J, Burkemper B, Jiang X, et al. Ocular biometric determinants of dark-to-light change in angle width: the Chinese American Eye Study. *Am J Ophthalmol*. 2022;237:183–192.

21. Quigley HA. The iris is a sponge: a cause of angle closure. *Ophthalmology*. 2010;117(1):1–2.

22. Quigley HA. Angle-closure glaucoma-simpler answers to complex mechanisms: LXVI Edward Jackson Memorial Lecture. *Am J Ophthalmol*. 2009;148(5):657–669, doi:10.1016/J.AJO.2009.08.009

23. Varma R, Hsu C, Wang D, Torres M, Azen SP. The Chinese American Eye Study: design and methods. *Ophthalmic Epidemiol*. 2013;20(6):335–347.

24. Xu BY, Israelsen P, Pan BX, Wang D, Jiang X, Varma R. Benefit of measuring anterior segment structures using an increased number of optical coherence tomography images: the Chinese American Eye Study. *Invest Ophthalmol Vis Sci*. 2016;57(14):6313–6319.

25. Shan J, Pardeshi A, Jiang X, et al. Optimal number and orientation of anterior segment OCT images to measure ocular biometric parameters in angle closure eyes: the Chinese American Eye Study. *Br J Ophthalmol*. Published online January 21, 2022, bjophthalmol-2021-319275, doi:10.1136/bjophthalmol-2021-319275.

26. Leung CKS, Weinreb RN. Anterior chamber angle imaging with optical coherence tomography. *Eye Lond Engl*. 2011;25(3):261–267.

27. Mansouri M, Ramezani F, Moghimi S, et al. Anterior segment optical coherence tomography parameters in phacomorphic angle closure and mature cataracts. *Invest Ophthalmol Vis Sci*. 2014;55(11):7403–7409.

28. Xu BY, Chiang M, Pardeshi AA, Moghimi S, Varma R. Deep neural network for scleral spur detection in anterior segment OCT images: the Chinese American Eye Study. *Transl Vis Sci Technol*. 2020;9(2):18.

29. Moghimi S, Chen R, Hamzeh N, Khatibi N, Lin SC. Qualitative evaluation of anterior segment in angle closure disease using anterior segment optical coherence tomography. *J Curr Ophthalmol*. 2016;28(4):170–175.

30. Sng CCA, Aquino MCD, Liao J, et al. Pretreatment anterior segment imaging during acute primary angle closure: insights into angle closure mechanisms in the acute phase. *Ophthalmology*. 2014;121(1):119–125.

31. Kumar RS, Tantisevi V, Wong MH, et al. Plateau iris in Asian subjects with primary angle closure glaucoma. *Arch Ophthalmol Chic Ill 1960*. 2009;127(10):1269–1272.

32. Baskaran M, Kumar RS, Friedman DS, et al. The Singapore Asymptomatic Narrow Angles Laser Iridotomy Study: five-year results of a randomized controlled trial. *Ophthalmology*. 2022;129(2):147–158.

33. He M, Jiang Y, Huang S, et al. Laser peripheral iridotomy for the prevention of angle closure: a single-centre, randomised controlled trial. *Lancet Lond Engl*. 2019;393(10181):1609–1618.

34. Xu BY, Liang S, Pardeshi AA, et al. Differences in ocular biometric measurements among subtypes of primary angle closure disease: the Chinese American Eye Study. *Ophthalmol Glaucoma*. 2021;4(2):224–231.